

Effect of Helical Trajectories of Electrons in Strongly Magnetized Plasmas on the Width of Hydrogen/Deuterium Spectral Lines: Beyond the Perturbation Theory

EUGENE OKS*

Physics Department, 206 Allison Lab., Auburn University, Auburn, AL 36849, USA

*Email: oksevgu@auburn.edu

ABSTRACT: The effects of *helical* trajectories of the perturbing electrons in magnetized plasmas on the dynamical Stark width of hydrogen or deuterium spectral lines has been studied analytically in our previous two papers – specifically in the situation where the magnetic field B is so strong that the dynamical Stark width of these lines reduces to the so-called adiabatic Stark width because the so-called nonadiabatic Stark width is completely suppressed. This situation corresponds, for example, to DA and DBA white dwarfs. We obtained those analytical results by using the formalism of the so-called conventional (or standard) theory of the impact Stark broadening: namely, by performing calculations in the second order of the Dyson *perturbation* expansion. The primary outcome was that the dynamical Stark broadening was found to not depend on the magnetic field B (for sufficiently strong B). In the present paper, in the spirit of the generalized theory of the dynamical Stark broadening we perform the corresponding *non-perturbative* analytical calculations equivalent to accounting for all order of the Dyson *perturbation* expansion. The results differ from our previous ones not only quantitatively, but – most importantly – qualitatively: namely, the dynamical Stark broadening does depend on the magnetic field B even for strong B . These results should be important for revising the interpretation of the hydrogen Balmer lines observed from DA and DBA white dwarfs. We also address some false statements in the literature on this subject.

Keywords: strongly magnetized plasmas; white dwarfs; Stark broadening; helical trajectories; non-perturbative analytical calculations; adiabatic width

1. INTRODUCTION

The effects of *helical* trajectories of the perturbing electrons in magnetized plasmas on the dynamical Stark width of hydrogen or deuterium spectral lines has been studied analytically in papers [1, 2] – specifically in the situation where the magnetic field B is so strong that the dynamical Stark width of these lines reduces to the so-called adiabatic Stark width because the so-called nonadiabatic Stark width is completely suppressed. This situation corresponds, for example, to DA and DBA white dwarfs. The analytical results were obtained in papers [1, 2] by using the formalism of the so-called conventional (or standard) theory of the impact Stark broadening [3, 4]: namely, by performing calculations in the second order of the Dyson *perturbation* expansion. The primary outcome was that the dynamical Stark broadening was found not to depend on the magnetic field B (for sufficiently strong B).

In the present paper, in the spirit of the generalized theory of the dynamical Stark broadening [5-7] we perform the corresponding *non-perturbative* analytical calculations equivalent to accounting for all order of the Dyson *perturbation* expansion. The results differ from those obtained in papers [1, 2] not only quantitatively, but – most importantly – qualitatively: namely, the dynamical Stark broadening does depend on the magnetic field B even for strong B .

2. SUMMARY OF STARTING FORMULAS FROM PAPERS [1, 2]

1. The radius-vector $\mathbf{R}(t)$ of a perturbing electron traveling on a helical trajectory in a magnetized plasma is

$$\mathbf{R}(t) = v_z \mathbf{t} \mathbf{B} / B + \boldsymbol{\rho} [1 + (r_{Bp} / \rho) \cos(\omega_B t + \varphi)] + \boldsymbol{\rho} \times \mathbf{B} [r_{Bp} / (\rho B)] \sin(\omega_B t + \varphi). \quad (1)$$

In Eq. (1), $\boldsymbol{\rho}$ is the impact parameter vector and $\boldsymbol{\rho} \times \mathbf{B}$ is its cross-product (vector product) with the magnetic field \mathbf{B} ; v_z is the component of the electron velocity parallel to \mathbf{B} . Other notations:

$$r_{Bp} = v_p / \omega_B, \quad \omega_B = eB / (m_e c). \quad (2)$$

In Eq. (2), ω_B is the Larmor frequency and v_p is the component of the electron velocity perpendicular to \mathbf{B} .

2. The electric field created by the perturbing electron at the location of the radiating hydrogen or deuterium atom:

$$\mathbf{E}(t) = e\mathbf{R}(t) / [R(t)]^3. \quad (3)$$

The z-projection of this electric field is:

$$E_z(t) = e(v_z t) / [\rho^2 + v_z^2 t^2 + v_p^2 / \omega_B^2 + 2(\rho v_p / \omega_B) \cos(\omega_B t + \varphi)]^{3/2}, \quad (4)$$

3. The nonadiabatic contribution to the dynamical Stark width, i.e., the contribution cause by the component of the field $\mathbf{E}(t)$ perpendicular to \mathbf{B} , is completely suppressed if

$$B > B_{cr} = 2T_e / (3|X_{\alpha\beta}|e\lambda_c) = 9.2 \times 10^2 T_e (\text{eV}) / |X_{\alpha\beta}| \text{ Tesla}, \quad (5)$$

where $\lambda_c = \hbar / (m_e c) = 2.426 \times 10^{-10}$ cm is the Compton wavelength of electrons. In Eq. (5), T_e is the electron temperature, and

$$X_{\alpha\beta} = |n_a(n_1 - n_2)_\alpha - n_b(n_1 - n_2)_\beta|. \quad (6)$$

In Eq. (6), n is the principal quantum numbers, and n_1 and n_2 are the parabolic quantum numbers of the upper (α) and lower (β) Stark states involved in the radiative transition.

4. The adiabatic part Φ_{ad} of the electron broadening operator Φ_{ab} (and the corresponding Stark width) is controlled by $E_z(t)$ given by Eq. (4).

5. For helical trajectories of perturbing electrons, the starting formula for the adiabatic Stark width $\Gamma_{\alpha\beta} = -\text{Re}[\langle \Phi_{ad} \rangle_{\beta\alpha}]$ for the line component, corresponding to the radiative transition between the upper Stark sublevel α and the lower Stark sublevel β , is

$$\Gamma_{\alpha\beta, \text{hel}} = N_e \int dv_z f_1(v_z) \int dv_p f_2(v_p) (v_z^2 + v_p^2)^{1/2} \sigma(v_z, v_p). \quad (7)$$

In Eq. (7), $f_2(v_p)$ is the two-dimensional Maxwell distribution and $f_1(v_z)$ is its one-dimensional counterpart. The operator $\sigma(v_z, v_p)$ discussed below has the physical meaning of the cross-section of the ‘‘optical’’ collisions causing the dynamical Stark broadening of the spectral line.

3. NON-PERTURBATIVE ANALYTICAL CALCULATIONS

In the generalized theory of the dynamical Stark broadening of hydrogenic spectral lines and its applications, the adiabatic contribution was calculated exactly, nonperturbatively (rather than in the second order of the Dyson perturbation expansion) [5-7]. This was achieved along the lines of the so-called old adiabatic theory – see, e.g., papers [8, 9]. In the formalism of the old adiabatic theory, the cross section σ of the optical collisions has the form:

$$\sigma = 2\pi \int_0^\infty d\rho \rho \langle 1 - \cos[\int_{-\infty}^\infty dt d_z E_z(t) / \hbar] \rangle. \quad (8)$$

In Eq. (8), the symbol $\langle \dots \rangle$ stands for the average over angular or phase variables; d_z is the matrix element of the z-projection of the electric dipole moment:

$$d_z/\hbar = 3X_{\alpha\beta}\hbar/(2m_e e). \quad (9)$$

The integral over time in Eq. (8) vanishes for the odd part of $E_z(t)$. Thus, it suffices performing the integration only for the even part $E_{z,\text{even}}(t)$ of $E_z(t)$:

$$E_z(t)_{\text{even}} = [E_z(t) + E_z(-t)]/2. \quad (10)$$

The latter was calculated in papers [1, 2] as follows.

The integral over the impact parameter ρ was broken in two parts

$$\sigma = \sigma_1 + \sigma_2, \quad (11)$$

σ_1 corresponding to the integral from ρ_0 to infinity and σ_2 corresponding to the integral from zero to ρ_0 , where

$$\rho_0 = v_p/\omega_B. \quad (12)$$

For calculating σ_1 , $E_{z,\text{even}}(t)$ was expanded in terms of the small parameter $\rho_0/\rho = v_p/(\omega_B\rho)$. After keeping the first non-vanishing term of the expansion, there was obtained:

$$E_z(t)_{\text{even}} = (\sin\varphi) (3e\rho v_p v_z/\omega_B) t[\sin(\omega_B t)]/(\rho^2 + v_z^2 t^2)^{5/2}. \quad (13)$$

For calculating σ_2 , $E_{z,\text{even}}(t)$ was expanded in terms of the small parameter $\rho/\rho_0 = \omega_B\rho/v_p$. After keeping the first non-vanishing term of the expansion, there was obtained:

$$E_z(t)_{\text{even}} = (\sin\varphi) (3e\rho v_p v_z/\omega_B) t[\sin(\omega_B t)]/(v_p^2/\omega_B^2 + v_z^2 t^2)^{5/2}. \quad (14)$$

Using expressions (13) and (14), obtained in papers [1, 2], we proceed now to calculating

$$\sigma_1 = 2\pi \int_{\rho_0}^{\infty} d\rho \rho \langle 1 - \cos[\int_{-\infty}^{\infty} dt d_z E_z(t)_{\text{even}}/\hbar] \rangle \quad (15)$$

and

$$\sigma_2 = 2\pi \int_0^{\rho_0} d\rho \rho \langle 1 - \cos[\int_{-\infty}^{\infty} dt d_z E_z(t)_{\text{even}}/\hbar] \rangle. \quad (16)$$

For σ_1 , after calculating the integral over time, the expression withing the symbol $\langle \dots \rangle$ in Eq. (15) becomes

$$1 - \cos[(\sin\varphi)3X_{\alpha\beta}\hbar v_p \omega_B K_1(\omega_B \rho/|v_z|)/(m_e |v_z|^3)], \quad (17)$$

where $K_1(s)$ is the modified Bessel function of the 2nd kind. Then the averaging of the expression (17) over φ yields

$$\langle \dots \rangle = 1 - J_0[3X_{\alpha\beta}\hbar v_p \omega_B K_1(\omega_B \rho/|v_z|)/(m_e |v_z|^3)], \quad (18)$$

where $J_0(u)$ is the Bessel function. For the range of ρ under consideration, the Bessel function $K_1(\omega_B \rho/|v_z|)$ is exponentially small, so that the argument of the Bessel function $J_0[\dots]$ is much smaller than unity. Therefore, Eq. (18) can be simplified to:

$$\langle \dots \rangle \approx [3X_{\alpha\beta}\hbar v_p \omega_B K_1(\omega_B \rho/|v_z|)/(2m_e |v_z|^3)]^2. \quad (19)$$

Then the integration over impact parameters in Eq. (15) yields:

$$\sigma_1 \approx (\pi/4)^{3/2} [3X_{\alpha\beta}\hbar v_p/(m_e v_z^2)]^2 \text{MeijerG}[\{\{\}, \{3/2\}\}, \{\{0, 0, 2\}, \{\}, \{v_p^2/v_z^2\}\}], \quad (19)$$

where $\text{MeijerG}[\dots]$ is the Meijer G-function.

Equation (19) for σ_1 coincides with σ_1 from papers [1, 2]. It does not depend on the magnetic field B (provided that B satisfies the condition (5)). However, below it is shown that our nonperturbative result for σ_2 significantly differs – both quantitatively and qualitatively – from the perturbatively-obtained result for σ_2 from papers [1, 2]. In particular, our nonperturbative result depends on the magnetic field B, while the perturbative result from papers [1, 2] did not depend on B.

For σ_2 , after calculating the integral over time, the expression within the symbol $\langle \dots \rangle$ in Eq. (16) becomes:

$$1 - \cos[(\sin\varphi)3X_{\alpha\beta}\hbar v_p \omega_B^2 K_1(v_p/|v_z|) \rho / (m_e |v_z|^3)]. \quad (20)$$

Then the averaging of the expression (20) over φ yields

$$\langle \dots \rangle = 1 - J_0[3X_{\alpha\beta}\hbar v_p \omega_B^2 K_1(v_p/|v_z|) \rho / (m_e |v_z|^3)]. \quad (21)$$

The subsequent integration over impact parameters in Eq. (21) leads to the following result for σ_2 :

$$\sigma_2 = (\pi v_p^2 / \omega_B^2) [1 - J_1(w)/w], \quad w = 3X_{\alpha\beta}\hbar v_p \omega_B K_1(v_p/|v_z|) / (m_e |v_z|^3). \quad (22)$$

Obviously, σ_2 depends on ω_B and thus on the magnetic field B.

For presenting the results in plots, we calculate the effective average values $\langle v_p \rangle$ and $\langle |v_z| \rangle$, as well as their ratio, as follows (compare to Eq. (7)):

$$\langle v_p \rangle = \int_{-\infty}^{\infty} dv_z f_1(v_z) \int_0^{\infty} dv_p f_2(v_p) (v_z^2 + v_p^2)^{1/2} v_p, \quad (23)$$

$$\langle |v_z| \rangle = \int_{-\infty}^{\infty} dv_z f_1(v_z) \int_0^{\infty} dv_p f_2(v_p) (v_z^2 + v_p^2)^{1/2} |v_z|. \quad (24)$$

As a result, we find:

$$\langle v_p \rangle = 1.60 \langle v_T \rangle, \quad \langle |v_z| \rangle = 0.665 \langle v_T \rangle, \quad \langle v_p \rangle / \langle |v_z| \rangle = 2.41, \quad (25)$$

where $v_T = (2T_e/m_e)^{1/2}$ is the mean thermal velocity of plasma electrons. Then we use these effective average values in Eq. (19) for σ_1 and in Eq. (22) for σ_2 in the subsequent plots where all quantities will be in atomic units.

Figure 1 displays the dependence of the ratio $\Gamma/(N_e v_T)$ on the Larmor frequency ω_B for the mean thermal velocity of electrons $v_T = 0.2$ a.u., corresponding to 2.7 eV, for $X_{\alpha\beta} = 6$ (solid line), $X_{\alpha\beta}$ being defined in Eq. (9). The corresponding perturbative result from papers [1, 2] is shown by the dashed line. We note that $X_{\alpha\beta} = 6$ corresponds to either $n_a = 3, (n_1 - n_2)_\alpha = 2, n_b = 1$ (which is a component of the Ly-beta line), or to $n_a = 4, (n_1 - n_2)_\alpha = 2, n_b = 2, (n_1 - n_2)_\beta = 1$, (which is a component of the Balmer-beta line), or to $n_a = 4, (n_1 - n_2)_\alpha = 3, n_b = 3, (n_1 - n_2)_\beta = 2$, (which is a component of the Paschen-alpha line), or to $n_a = 6, (n_1 - n_2)_\alpha = 1, n_b = 1$, (which is a component of Lyman-epsilon line), or to $n_a = 6, (n_1 - n_2)_\alpha = 2, n_b = 3, (n_1 - n_2)_\beta = 2$, (which is a component of the Paschen-gamma line), or to $n_a = 4, (n_1 - n_2)_\alpha = 2, n_b = 3, (n_1 - n_2)_\beta = 2$, (which is a component of the Paschen-alpha line), or to $n_a = 6, (n_1 - n_2)_\alpha = 3, n_b = 4, (n_1 - n_2)_\beta = 3$, (which is a component of the Brackett-beta line). Thus, the value of $X_{\alpha\beta} = 6$ represents Stark components of seven spectral lines, which is why we chose this value for Fig. 1.

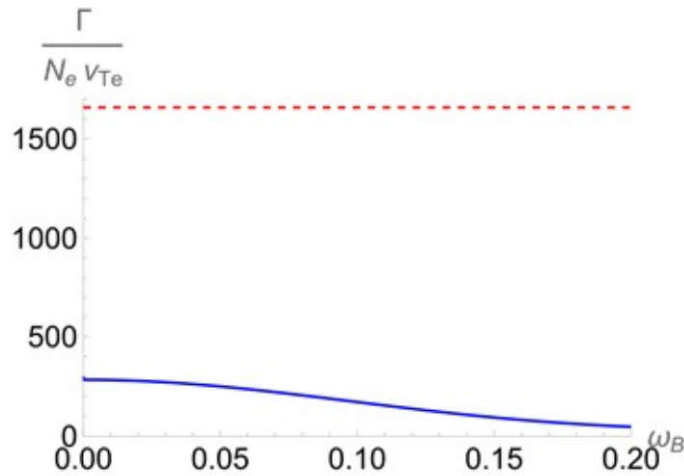


Fig. 1. Dependence of the ratio $\Gamma/(N_e v_T)$ on the Larmor frequency ω_B for the mean thermal velocity of electrons $v_T = 0.2$ a.u., corresponding to 2.7 eV, for $X_{\alpha\beta} = 6$ (solid line). The corresponding perturbative result from papers [1, 2] is shown by the dashed line. All quantities are in atomic units.

From Fig. 1 it is seen that the perturbative calculation from papers [1, 2] overestimated the Stark width. It also illustrates that the perturbative calculation from papers [1, 2] did not produce any dependence of the Stark with on the magnetic field, while the nonperturbative (more accurate calculation) demonstrates a significant dependence of the Stark width on the magnetic field.

4. CONCLUSIONS

We continued studying analytically how the dynamical Stark width of hydrogen or deuterium spectral lines is affected by the *helical* (rather than rectilinear) trajectories of the perturbing electrons in magnetized plasmas – specifically where the magnetic field B is so strong that the dynamical Stark width of these lines reduces to the so-called adiabatic Stark width because the so-called nonadiabatic Stark width is completely suppressed. In distinction to our previous papers [1, 2], where the corresponding analytical calculations were done in the second order of the Dyson *perturbation* expansion, in the present paper we performed *non-perturbative* analytical calculations equivalent to accounting for all order of the Dyson perturbation expansion in the spirit of the generalized theory of the dynamical Stark broadening [5-7].

The results of the present paper differ from those obtained in papers [1, 2] not only quantitatively, but – most importantly – qualitatively: namely, the dynamical Stark broadening does depend on the magnetic field B even for strong B , while in papers [1, 2] the dynamical Stark broadening did not depend on B . The results of the present paper should be important for revising the interpretation of the hydrogen Balmer lines observed from DA and DBA white dwarfs.

According to observations, the magnetic field in plasmas of white dwarfs can range from 10^3 Tesla to 10^5 Tesla (see, e.g., papers [10-27] listed in the chronological order and references therein), thus easily exceeding the critical value from Eq. (5). Indeed, for the typical electron temperature $T_e \sim 1$ eV in the white dwarfs plasmas emitting hydrogen lines, Eq. (5) yields $B_{cr} \sim 10^3/|X_{\alpha\beta}|$ Tesla $< 10^3$ Tesla.

We note in passing that Alexiou in his paper [28], which was limited to simulations of the same effect, made several false statements about the analytical results of our paper [1] – see details in Appendix A. This is the continuation of a long line of his false statements and of his misunderstanding of the underlying physics. For example, Alexiou demonstrated the total lack of understanding the physics behind the area of the intra-Stark spectroscopy. Namely, he published simulations [29] where he totally ignored the actual nature of the Langmuir-wave-caused dips and thus was unable to reproduce them for the experimental spectral line profiles from papers [30, 31]: the papers describing the projects on spectroscopic diagnostics of the relativistic laser-plasma interactions – the projects resulting from the collaboration of experimentalists and theorists from seven countries (Japan, the UK, France, Germany,

Hungary, the USA, and Russia). Specific flaws of Alexiou simulations [29] have been described in paper [32].

Actually, Alexiou has a long history of failures of his code to reproduce important experimental results. For example: compared to the widths of the Balmer-alpha line, measured in the benchmark experiment in the Kunze's group [33], Alexiou's simulations [34] dramatically underestimated the measured width – by 30% for the lowest density. (In the benchmark experiment [33], plasma parameters were measured by the Thomson scattering independently of the measurements of the line profiles.) Instead of trying to find out what is wrong with his simulations, Alexiou suggested that this benchmark experiment is incorrect – the statement typical for him. However, physics is first and foremost the experimental science, rather than the “simulational” science – especially regarding precise, benchmark experiments performed in rigorously controlled conditions (such as, e.g., the experiment [33]). Typically, the benchmark experiments, rather than simulations, move physics to new horizons.

Alexiou does not disdain making false statements about the pioneering works of others to promote his simulations that are actually of the secondary importance.

Appendix A. False statements from Alexiou paper [28]

1. The effect of helical trajectories of the perturbing electrons on the Stark width of hydrogen line was first presented in our paper [1] and then represented in our review [2]. The analytical results from paper [1] were obtained in frames of the so-called conventional (or standard) theory of the impact Stark broadening [3, 4]. Despite this, Alexiou [28] falsely stated that the results in paper [1] were obtained in frames of the so-called generalized theory of Stark broadening. This ridiculous statement by Alexiou is the first example of his reading failure.
2. The most important: Alexiou [28] falsely stated that presumably in paper [1] there was predicted analytically that the allowance for Helical Trajectories of the Perturbing Electrons (HTPE) leads to a dramatic width increase of the lines Balmer-beta, Balmer-delta, and Balmer-epsilon at high densities, while his simulations yielded a decrease of the corresponding widths. For supporting his false statement, Alexiou used specific examples of the Balmer-beta, Balmer-delta, and Balmer-epsilon lines at the electron temperature $T_e = 1$ eV and the electron density $N_e = 2 \times 10^{17}$ cm⁻³.

However, in reality, according to Eqs. (18) and (47), and Fig. 1 from paper [1], whether the allowance for HTPE increases or decreases the width of the Stark components of any hydrogen line, depends on the value of the following dimensionless parameter

$$D = 5.57 \times 10^{-11} |X_{\alpha\beta}| [N_e(\text{cm}^{-3})]^{1/2} / T_e(\text{eV}), \quad (\text{A.1})$$

where

$$X_{\alpha\beta} = n_a q_\alpha - n_b q_\beta, \quad q_\alpha = (n_1 - n_2)_\alpha, \quad q_\beta = (n_1 - n_2)_\beta. \quad (\text{A.2})$$

In Eq. (A.2), n is the principal quantum number, n_1 and n_2 are the parabolic quantum numbers (while q is often called the electric quantum number); we noted in [1] that $X_{\alpha\beta}$ is the standard label of the Stark component of hydrogen or deuterium spectral lines corresponding to the radiative transition between the upper (α) and lower (β) Stark sublevels. According to Eq. (47) and Fig. 1 from paper [1], the allowance for HTPE increases the width of a Stark component if $D > 0.44$, but decreases its width if $D < 0.44$.

For the plasma parameters chosen by Alexiou, Eq. (A.1) simplifies to

$$D = 0.025 |X_{\alpha\beta}|. \quad (\text{A.3})$$

The critical value of $D = 0.44$ corresponds in this case to the critical value of $|X_{\alpha\beta}| = 18$, so that according to paper [1], *the allowance for HTPE increases the width of Stark components having $|X_{\alpha\beta}| > 18$, but decreases the width of Stark components having $|X_{\alpha\beta}| < 18$.*

For the Balmer-beta line, all intense Stark components have $|X_{\alpha\beta}|$ of no more than 10. So, the actual prediction from paper [1] for the Balmer-beta line at the plasma parameters chosen by Alexiou is the *decrease* of the Stark width (what can be also seen from Figs. 2 and 3 from paper [1]), rather than the increase of the Stark width falsely stated by Alexiou. This is another example of Alexiou's reading failure.

For the Balmer-delta line, the most intense Stark component has $|X_{\alpha\beta}| = 6$. So, based on the results from paper [1], for the plasma parameters chosen by Alexiou, one should *not expect the increase* of the Stark width – contrary to Alexiou's false statement.

For the Balmer-epsilon line, the most intense Stark component has $|X_{\alpha\beta}| = 14$. So, again, based on the results from paper [1], for the plasma parameters chosen by Alexiou, one should *not expect the increase* of the Stark width – contrary to Alexiou's false statement.

The statements from paper [1] concerning the increase of the Stark width of the Balmer-delta and higher lines due to HTPe related to the electron densities $N_e > 10^{18} \text{ cm}^{-3}$, i.e., electron densities much higher than the one value of N_e chosen by Alexiou in his simulations [28]. This situation is yet another demonstration of the superiority of analytical results over simulations: the analytical results are valid for a broad range of the electron density, while Alexiou performed the simulations for only one value of the electron density.

3. Last but not least: according to Eq. (27) from paper [1], the analytical results presented in that paper are valid for

$$B(\text{Tesla}) \gg B_{\text{cr}} = 650T_e(\text{eV})/|X_{\alpha\beta}|. \quad (\text{A.4})$$

For the temperature $T = 1 \text{ eV}$, chosen by Alexiou for his simulations, the critical magnetic field is

$$B_{\text{cr}} = 650\text{Tesla} = 650/|X_{\alpha\beta}|. \quad (\text{A.5})$$

Alexiou performed his simulations for the following three values of the magnetic field: 300, 500, and 2000 Tesla. For the Balmer-beta line, the most intense component has $|X_{\alpha\beta}| = 4$, so that $B_{\text{cr}} = 160 \text{ Tesla}$. Therefore, for $B = 300 \text{ Tesla}$, the ratio $B/B_{\text{cr}} = 1.9$ is *not* much greater than unity. Similarly, for $B = 500 \text{ Tesla}$, the ratio $B/B_{\text{cr}} = 3.1$ is *not* much greater than unity. Thus, for $B = 300 \text{ Tesla}$ and $B = 500 \text{ Tesla}$, there are actually no analytical predictions from paper [1]. Therefore, Alexiou's comparison of his simulations in this case with presumed "predictions from paper [1]" is the next example of his reading failure.

For the Balmer-delta line, the most intense component has $|X_{\alpha\beta}| = 6$, so that $B_{\text{cr}} = 110 \text{ Tesla}$. Therefore, for $B = 300 \text{ Tesla}$, the ratio $B/B_{\text{cr}} = 2.7$ is *not* much greater than unity. Thus, for $B = 300 \text{ Tesla}$, there are actually no analytical predictions from paper [1]. Therefore, Alexiou's comparison of his simulations in this case with presumed "predictions from paper [1]" is yet another example of his reading failure. (We also note that for $B = 500 \text{ Tesla}$, the ratio $B/B_{\text{cr}} = 4.5$, so that the corresponding results from paper [1] would have a significant error margin in this case, so that comparing them with Alexiou's simulations is meaningless.)

References

1. Oks, E. Effect of Helical Trajectories of Electrons in Strongly Magnetized Plasmas on the Width of Hydrogen/Deuterium Spectral Lines: Analytical Results and Applications to White Dwarfs. *Intern. Review of Atomic and Molecular Phys.* **2017**, *8*, 61-72.
2. Oks, E. Review of Recent Advances in the Analytical Theory of Stark Broadening of Hydrogenic Spectral Lines in Plasmas: Applications to Laboratory Discharges and Astrophysical Objects. *Atoms* **2018**, *6*, 50; Erratum, *Atoms* **2019**, *7*, 68.
3. Kepple, P., Griem, H.R. Improved Stark Profile Calculations for the Hydrogen Lines H α , H β , H γ and H δ . *Phys. Rev.* **1968**, *173*, 317.
4. Griem, H.R. *Spectral Line Broadening by Plasmas*; Academic: New York, 1974.
5. Ispolatov, Ya., Oks, E. A Convergent Theory of Stark Broadening of Hydrogen Lines in Dense Plasmas. *J. Quant. Spectr. Rad. Transfer* **1994**, *51*, 129-138.
6. Oks, E., Derevianko, A., Ispolatov, Ya. A Generalized Theory of Stark Broadening of Hydrogen-Like Spectral Lines in Dense Plasmas. *J. Quant. Spectr. Rad. Transfer* **1995**, *54*, 307-316.
7. Oks, E. Stark Widths of Hydrogen Spectral Lines in Plasmas: a Highly-Advanced Non-Simulative Semiclassical Theory and Tables. AIP

- Conf. Proc. **2006**, 874, 19-34.
8. Anderson, P.W. A Method of Synthesis of the Statistical and Impact Theories of Pressure Broadening. *Phys. Rev.* **1952**, 86, 809.
 9. Lisitsa, V.S. Stark Broadening of Hydrogen Lines in Plasmas. *Sov. Phys. Uspekhi* **1977**, 122, 603-630.
 10. Angel, J.R.P. Magnetic White Dwarfs. *Ann. Rev. Astron. Astrophys.* **1978**, 16, 487-519.
 11. Angel, J. R. P., Liebert, J., Stockman, H. S. The Optical Spectrum of Hydrogen at 160-350 Million Gauss in the White Dwarf GRW +70 deg 8247. *Astrophys. J., Part 1* **1985**, 292, 260-266.
 12. Wunner, G., Roesner, W., Herold, H., Ruder, H. Stationary Hydrogen Lines in White Dwarf Magnetic Fields and the Spectrum of the Magnetic Degenerate GRW +70 8247. *Astron. Astrophys.* **1985**, 149, 102-108.
 13. Henry, R.J.W., Oconnell, R.F. Hydrogen Spectrum in Magnetic White Dwarfs: H α , H β , and H γ Transitions. *Publ. Astron. Soc. Pacific* **1985**, 97, 333-339.
 14. Bergeron, P., Wesemael, F., Fontaine, G., Liebert, J. On the Surface Composition of Cool, Hydrogen-Line White Dwarfs: Discovery of Helium in the Atmospheres of Cool DA Stars and Evidence for Convective Mixing. *Astrophys. J.* **1990**, 351, L21-L24.
 15. MacDonald, J., Vennes, S. How Much Hydrogen is There in a White Dwarf? *Astrophys. J., Part 1* **1991**, 371, 719-738.
 16. Bergeron, P., Saffer, R.A., Liebert, J. A Spectroscopic Determination of the Mass Distribution of DA White Dwarfs. *Astrophys. J.* **1992**, 394, 228-247.
 17. Fassbinder, P., Schweizer, W. Stationary Hydrogen Lines in Magnetic and Electric Fields of White Dwarf Stars. *Astron. Astrophys.* **1996**, 314, p.700-706.
 18. Reimers, D., Jordan, S., Koester, D., Bade, N. Discovery of Four White Dwarfs with Strong Magnetic Fields by the Hamburg/ESO Survey. *Astron. Astrophys.* **1996**, 311, 572.
 19. Kowalski, P.M., Saumon, D. Found: The Missing Blue Opacity in Atmosphere Models of Cool Hydrogen White Dwarfs. *Astrophys. J.* **2006**, 651, L137-L140.
 20. Kawka, A., Vennes, S., Schmidt, G.D., Wickramasinghe, D.T., Koch, R. Spectropolarimetric Survey of Hydrogen-Rich White Dwarf Stars. *Astrophys. J.* **2007**, 654, 499-520.
 21. Tremblay, P.-E., Bergeron, P. Spectroscopic Analysis of DA White Dwarfs: Stark Broadening of Hydrogen Lines Including Nonideal Effects. *Astrophys. J.* **2009**, 696, 1755-1770.
 22. Külebi, B., Jordan, S., Euchner, F., Gänsicke, B.T., Hirsch, H. Analysis of Hydrogen-Rich Magnetic White Dwarfs Detected in the Sloan Digital Sky Survey. *Astron. Astrophys.* **2009**, 506, 1341-1350.
 23. Gianninas, A., Bergeron, P., Ruiz, M.T. A Spectroscopic Survey and Analysis of Bright, Hydrogen-Rich White Dwarfs. *Astrophys. J.* **2011**, 743, 138.
 24. Franzon, B., Schramm, St. Effects of Magnetic Fields in White Dwarfs. *J. Phys. Conf. Ser.* **2017**, 861, 012015.
 25. Rolland, B., Bergeron, P., Fontaine, G. On the Spectral Evolution of Helium-atmosphere White Dwarfs Showing Traces of Hydrogen. *Astrophys. J.* **2018**, 857, 56.
 26. Bohlin, R.C., Hubeny, I., Rauch, T. New Grids of Pure-hydrogen White Dwarf NLTE Model Atmospheres and the HST/STIS Flux Calibration. *Astronom. J.* **2020**, 160, 21.
 27. Hardy, F., Dufour, P., Jordan, St. Spectrophotometric Analysis of Magnetic White Dwarf – I. Hydrogen-rich Compositions. *Monthly Notices of the Royal Astronomical Society* **2023**, 520, 6111-6134.
 28. Alexiou, S. Effects of Spiraling Trajectories on White Dwarf Spectra: High Rydberg States. *Atoms* **2023**, 11, 141.
 29. Alexiou, S. Analysis of Plasma Emission Experiments and ‘Dips’. *Atoms* **2023**, 11, 29.
 30. Oks, E.; Dalimier, E.; Faenov, A.Ya.; Angelo, P.; Pikuz, S.A.; Pikuz, T.A.; Skobelev, I.Yu.; Ryazanzev, S.N.; Durey, P.; Doehl, L.; Farley, D.; Baird, C.D.; Lancaster, K.L.; Murphy, C.D.; Booth, N.; Spindloe, C.; McKenna, P.; Neumann, N.; Roth, M.; Kodama, R.; Woolsey, N. In-Depth Study of Intra-Stark Spectroscopy in the X-Ray Range in Relativistic Laser-Plasma Interactions. *J. Phys. B: At. Mol. Opt. Phys.* **2017**, 50, 245006.
 31. Dalimier, E.; Pikuz, T.A.; Angelo, P. Mini-Review of Intra-Stark X-ray Spectroscopy of Relativistic Laser-Plasma Interactions. *Atoms* **2018**, 6, 45-59.
 32. Dalimier, E.; Oks, E.; Pikuz, T.; Angelo, P. The Myths and the Truth about Langmuir-Wave-Caused “Dips” in Spectral Line Profiles. *Intern. Review of Atom. Molec. Phys.* **2023**, 14, 81-88.
 33. Büscher, S.; Wrubel, Th.; Ferri, S.; Kunze, H.-J. The Stark Width and Shift of the Hydrogen H α Line. *J. Phys. B* **2002**, 35, 2889-2897.
 34. Alexiou, S. Stark Broadening of Hydrogen Lines in Dense Plasmas: Analysis of Recent Experiments. *Phys. Rev. E* **2005**, 71, 066403.